


Research Article

Angiotensin Receptor Blocker and Neprilysin Inhibitor Suppresses Cardiac Dysfunction by Accelerating Myocardial Angiogenesis in Apolipoprotein E-Knockout Mice Fed a High-Fat Diet

Yasunori Suematsu ¹, Kohei Tashiro,¹ Hidetaka Morita,¹ Akihito Ideishi,¹ Takashi Kuwano,¹ and Shin-ichiro Miura ^{1,2}

¹Department of Cardiology, Fukuoka University School of Medicine, Fukuoka, Japan

²Department of Cardiology, Fukuoka University Nishijin Hospital, Fukuoka, Japan

Correspondence should be addressed to Shin-ichiro Miura; miuras@cis.fukuoka-u.ac.jp

Received 27 March 2021; Accepted 8 July 2021; Published 4 August 2021

Academic Editor: Robert Speth

Copyright © 2021 Yasunori Suematsu et al. This is an open access article distributed under the Creative Commons Attribution License, which permits unrestricted use, distribution, and reproduction in any medium, provided the original work is properly cited.

Hypothesis. Myocardial angiogenesis is important for maintaining cardiac contractile function in patients with cardiac hypertrophy. Evidence shows that angiotensin receptor blocker and neprilysin inhibitors (ARNIs) improve heart failure. The present study investigated the myocardial angiogenic effect of valsartan plus sacubitril in early-stage cardiac dysfunction. **Materials and Methods.** Male apolipoprotein E-knockout mice fed a high-fat diet were divided into control (CTL), valsartan (30 mg/kg) (VAL), sacubitril (30 mg/kg) (SAC), and valsartan plus sacubitril (30 mg/kg each) (VAL/SAC) groups after 4 weeks of prefeeding and were subsequently treated for 12 weeks. **Results.** The VAL/SAC group exhibited significantly higher serum brain natriuretic peptide levels; more subtle changes in left ventricular systolic diameter, fractional shortening, and ejection fraction, and significantly higher expression levels of natriuretic peptide precursor B and markers of angiogenesis, including clusters of differentiation 34, vascular endothelial growth factor A, and monocyte chemoattractant protein 1, than the CTL group. **Conclusions.** Valsartan plus sacubitril preserved left ventricular systolic function in apolipoprotein E-knockout mice fed a high-fat diet. This result suggests that myocardial angiogenic factors induced by ARNI might provide cardioprotective effects.

1. Introduction

Obesity [1], hypertension [2], diabetes mellitus [3], and metabolic syndrome [4] can cause cardiac hypertrophy, leading to heart failure [5, 6]. Myocardial angiogenesis is necessary for maintaining cardiac systolic function during cardiac hypertrophy [7]. Under overload conditions, cardiomyocytes become hypertrophic and myocardial angiogenesis accelerates in response to an increased demand for oxygen. However, sustained cardiac hypertrophy causes maladaptation, cardiac remodeling, and heart failure [7]. Evidence shows that myocardial angiogenesis can help prevent heart failure progression, and therapeutic angiogenesis is an important issue in the field of cardiovascular disease

[8–10]. Nonetheless, optimal treatment protocols have yet to be established.

Neprilysin, also known as neutral endopeptidase, inactivates natriuretic peptides by cleaving a variety of peptide bonds [11]. Therefore, the valsartan/sacubitril combination serves as an angiotensin receptor blocker and neprilysin inhibitor (ARNI) [12], a type of medication that increases natriuretic peptide availability. The PARADIGM-HF clinical trials showed that the valsartan/sacubitril combination exhibited better cardioprotective effects against heart failure with reduced left ventricular ejection fraction (HFrEF) than angiotensin-converting enzyme inhibitors [13]. Moreover, the US and European guidelines for HF management recommend valsartan/sacubitril as first-line therapy for HFrEF

[14, 15]. Furthermore, clinical trials have shown that valsartan/sacubitril promoted better reduction in secondary functional mitral regurgitation than valsartan (PRIME) [16], with another a clinical trial investigating the effects of valsartan/sacubitril on ventricular remodeling (i.e., PROVE-HF) currently ongoing [17]. Basic studies confirmed the pleiotropic effects of ARNI. Accordingly, our previous studies reported that ARNI exhibited antifibrotic cardioprotective effects against diabetic HFREF [18], promoted antihypertrophic cardioprotective effects [19], improved renal function during chronic kidney disease [20], and suppressed aldosterone synthesis [21], and ARNI also affects pulmonary hypertension [22], endothelial dysfunction [23], and atherosclerotic plaque formation [24]. However, no study has yet investigated the effects of ARNI on myocardial angiogenesis in an early-stage cardiac dysfunction model. Therefore, the present study sought to determine whether valsartan plus sacubitril administration could improve cardiac dysfunction in an animal model of early-stage cardiac dysfunction.

2. Materials and Methods

2.1. Experimental Protocol. All experimental protocols were approved by the Animal Care and Use Committee of Fukuoka University and conformed to the Guide for the Care and Use of Laboratory Animals of the Institute of Laboratory Animal Resources.

Apolipoprotein E-knockout mice were purchased from Charles River Laboratories Japan, Inc., Japan. Apolipoprotein E-knockout mice with or without a high-fat diet reportedly exhibited cardiac dysfunction [25–28]. To establish a model of early-stage cardiac dysfunction, 8-week-old male apolipoprotein E-knockout mice were started on a high-fat diet (week 4) containing 0.5% cholesterol and 17% coconut oil with a normal chow diet. The proportions of calories from protein, fat, and nitrogen-free extract were 16.8%, 43.0%, and 40.2%, respectively. After 4 weeks of prefeeding, the mice were divided into control (CTL), valsartan (30 mg/kg) (VAL), sacubitril (30 mg/kg) (SAC), and valsartan plus sacubitril (30 mg/kg each) (VAL/SAC) groups (week 0). Drugs were administered by mixed drinking water. Body weight and blood pressure were measured every 4 weeks (weeks 4, 0, 4, 8, and 12). Blood pressure was measured through a tail cuff-based MK-2000 device (Muromachi Kikai Co., Ltd., Tokyo, Japan). Echocardiography was performed using isoflurane (2%–3%) at weeks 0 and 12. The drug dosages relied on previous basic research using valsartan and sacubitril [18–20, 22, 23]. Previous studies reported that male apolipoprotein E-knockout mice exhibited cardiac endothelial-mesenchymal transition after 8 weeks on a high-fat diet, starting from 8 weeks of age [27], and 7.5-month-old male apolipoprotein E-knockout mice exhibited endothelial dysfunction [25]. Therefore, our study investigated 8-week-old apolipoprotein E-knockout mice until they were 6 months old, during which early-stage cardiac dysfunction would have occurred based on the previous reports [25, 27]. After 12 weeks of treatment, we measured serum brain natriuretic peptide (BNP) levels with a RayBio Mouse BNP Enzyme Immunoassay Kit (Catalog #: EIAM-BNP,

TABLE 1: Primer sequences used in quantitative RT-PCR.

Gene		Sequence (5' to 3')
NPPA	Forward	GGGGGTAGGATTGACAGGAT
	Reverse	ACACACCACAAGGGCTTAGG
NPPB	Forward	TCCTAGCCAGTCTCCAGAGC
	Reverse	CCTTGGTCCTTCAAGAGCTG
TGF- β	Forward	GCTTCTAGTGCTGACGCCCG
	Reverse	GACTGGCGAGCCTTAGTTTG
MyH7	Forward	GAGGAGAGGGCGGACATC
	Reverse	GGAGCTGGGTAGCACAAAGAG
CD34	Forward	GACAACATGTGGTGGCTGAC
	Reverse	AGCTGAAGGCAGCATGAAGT
VEGFA	Forward	CAGGCTGCTGTAAACGATGAA
	Reverse	TATGTGGCTGGCTTTGGTGAG
MCP1	Forward	AGCACCAGCCAACTCTCACT
	Reverse	GGCGTTAACTGCATCTGGCT
ATP2a2	Forward	TACTGACCCTGTCCCTGACC
	Reverse	CACCACCCTCCCATAGCTT
VCAM-1	Forward	ACAGACAGTCCCCTCAATGG
	Reverse	ACCTCCACCTGGGTTCTCTT
β catenin	Forward	GTGCAATTCTGAGCTGACA
	Reverse	CTTAAAGATGGCCAGCAAGC
VE-cadherin	Forward	ACCTTTCAGATGCAGCGACT
	Reverse	TGGCACACCATCATCTTGTTTT
Nfkbia	Forward	TCGCTCTTGTGAAATGTGG
	Reverse	CTCTCGGGTAGCATCTGGAG
Ikkbb	Forward	GAGCTGTCCTTACCCTGCTG
	Reverse	TGCTGCAGAACGATGTTTTC
Ikkbg	Forward	TGAAGAAATGCCAACAGCAG
	Reverse	CTAAAGCTTGCCGATCCTTG
Lamp2	Forward	ATTTGGCTAATGGCTCAGCTT
	Reverse	GAAAGCACCTGCTCTTTGTTG
Pink1	Forward	TTGAGGAGCAGACTCCCAGT
	Reverse	AGTCCCCTCCACAAGGATG
β actin	Forward	CCACACCCGCCACCAGTTCG
	Reverse	TACAGCCCGGGGAGCATCGT

NPPA: natriuretic peptide type A; NPPB: natriuretic peptide type B; TGF- β : transforming growth factor-beta; MyH7: myosin heavy chain 7; CD34: clusters of differentiation 34; VEGFA: vascular endothelial growth factor A; MCP1: monocyte chemotactic protein 1; ATP2a2: gene name of sarcoplasmic/endoplasmic reticulum calcium adenosine triphosphatase 2; VCAM-1: vascular cell adhesion protein 1; VE-cadherin: vascular endothelial-cadherin; Nfkbia: nuclear factor-kappa B (NF- κ B) inhibitor alpha; Ikkbb: inhibitor of NF- κ B kinase subunit beta; Ikkbg: inhibitor of NF- κ B kinase regulatory subunit gamma; Lamp2: lysosome-associated membrane glycoprotein 2; Pink1: phosphatase and tensin homolog deleted on chromosome 10-induced kinase 1.

RayBiotech, GA, USA); the expression of messenger ribonucleic acid (mRNA) in the left ventricle was measured using reverse transcription-polymerase chain reaction (RT-PCR), and Masson's trichrome staining and clusters of differentiation 34 (CD34) immunostaining were performed in the left ventricle.

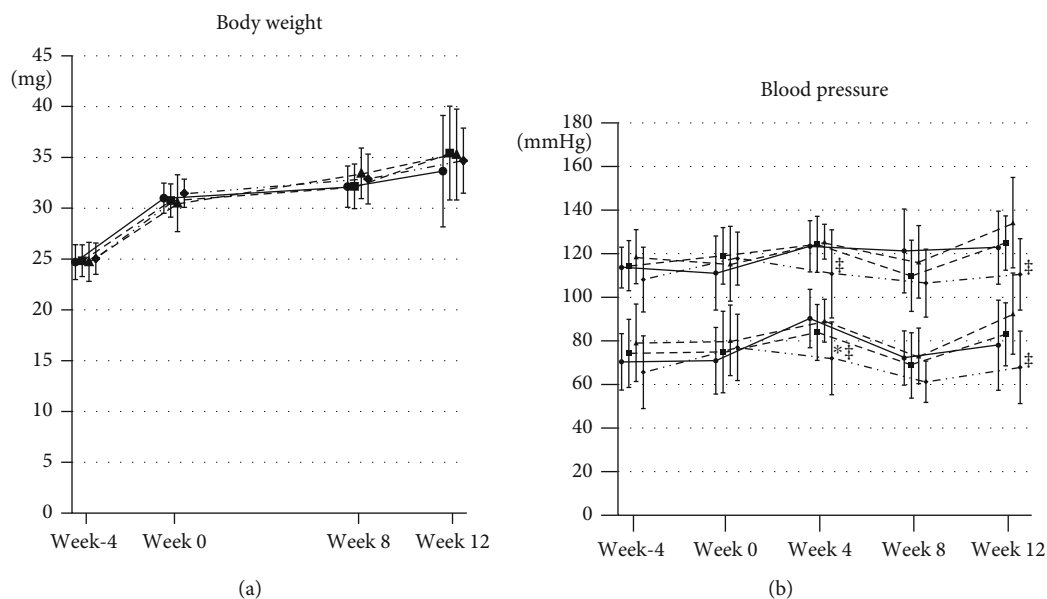


FIGURE 1: Changes in body weight and blood pressure. Changes in (a) body weight and (b) blood pressure, including systolic blood pressure and diastolic blood pressure in each group. CTL: control group; VAL: valsartan group; SAC: sacubitril group; VAL/SAC: valsartan plus sacubitril group. The round marker and solid line, square marker and dotted line, triangle marker and dashed line, and rhombus marker and chain line indicate CTL, VAL, SAC, and VAL/SAC. CTL ($n = 8$), VAL ($n = 7$), SAC ($n = 8$), and VAL/SAC ($n = 8$) were investigated. * and ‡ indicate significant differences compared with CTL and SAC during the same week, respectively.

TABLE 2: Cardiac functions by echocardiography in pre and posttreatment.

	CTL	VAL	SAC	VAL/SAC
Week 0				
HR	641 ± 76	636 ± 56	619 ± 84	596 ± 69
IVSTd	0.53 ± 0.09	0.54 ± 0.05	0.54 ± 0.12	0.53 ± 0.07
LVPWd	0.64 ± 0.13	0.66 ± 0.13	0.63 ± 0.05	0.68 ± 0.07
LVDd	3.6 ± 0.5	3.5 ± 0.4	3.6 ± 0.5	3.8 ± 0.4
LVDs	2.0 ± 0.4	1.9 ± 0.4	2.2 ± 0.3	2.3 ± 0.4
LVEF	81.6 ± 4.8	81.8 ± 5.3	79.4 ± 3.7	78.9 ± 5.3
LVFS	44.8 ± 5.1	44.8 ± 5.3	42.3 ± 3.8	41.9 ± 5.3
Week 12				
HR	551 ± 42	513 ± 45	518 ± 43	575 ± 48 ^{†‡}
IVSTd	0.70 ± 0.05	0.74 ± 0.05	0.78 ± 0.10*	0.71 ± 0.06
LVPWd	0.76 ± 0.09	0.87 ± 0.11*	0.84 ± 0.11	0.74 ± 0.07 ^{†‡}
LVDd	4.4 ± 0.3	4.2 ± 0.3	4.0 ± 0.5	4.3 ± 0.2
LVDs	2.9 ± 0.4	2.5 ± 0.3	2.4 ± 0.5*	2.6 ± 0.4
LVEF	67.8 ± 8.2	76.0 ± 7.2*	76.1 ± 7.5*	76.6 ± 6.7*
LVFS	33.3 ± 6.1	39.6 ± 6.4	39.6 ± 6.3	40.1 ± 6.1*

CTL: control group; VAL: valsartan group; SAC: sacubitril group; VAL/SAC: valsartan plus sacubitril group; HR: heart rate; IVSTd: interventricular septum thickness diameter; LVPWd: left ventricular posterior wall thickness diameter; LVDd: left ventricular internal dimension in diastole; LVDs: left ventricular internal dimension in systole; LVEF: left ventricular ejection fraction; LVFS: left ventricular fractional shortening. *, †, and ‡ show significant differences compared to CTL, VAL, and SAC, respectively.

2.2. Evaluation of Cardiac Function. Echocardiographic measurements were performed using NEMIO SSA-550A (Toshiba, Tokyo, Japan). From the short-axis two-dimensional view and M mode at the level of the papillary muscle, we measured heart rate, interventricular septum

thickness diameter (IVSTd), left ventricular internal dimension in diastole (LVDd), left ventricular posterior wall thickness diameter (LVPWd), left ventricular internal dimension in systole (LVDs), left ventricular ejection fraction (LVEF), and left ventricular fractional shortening (LVFS).

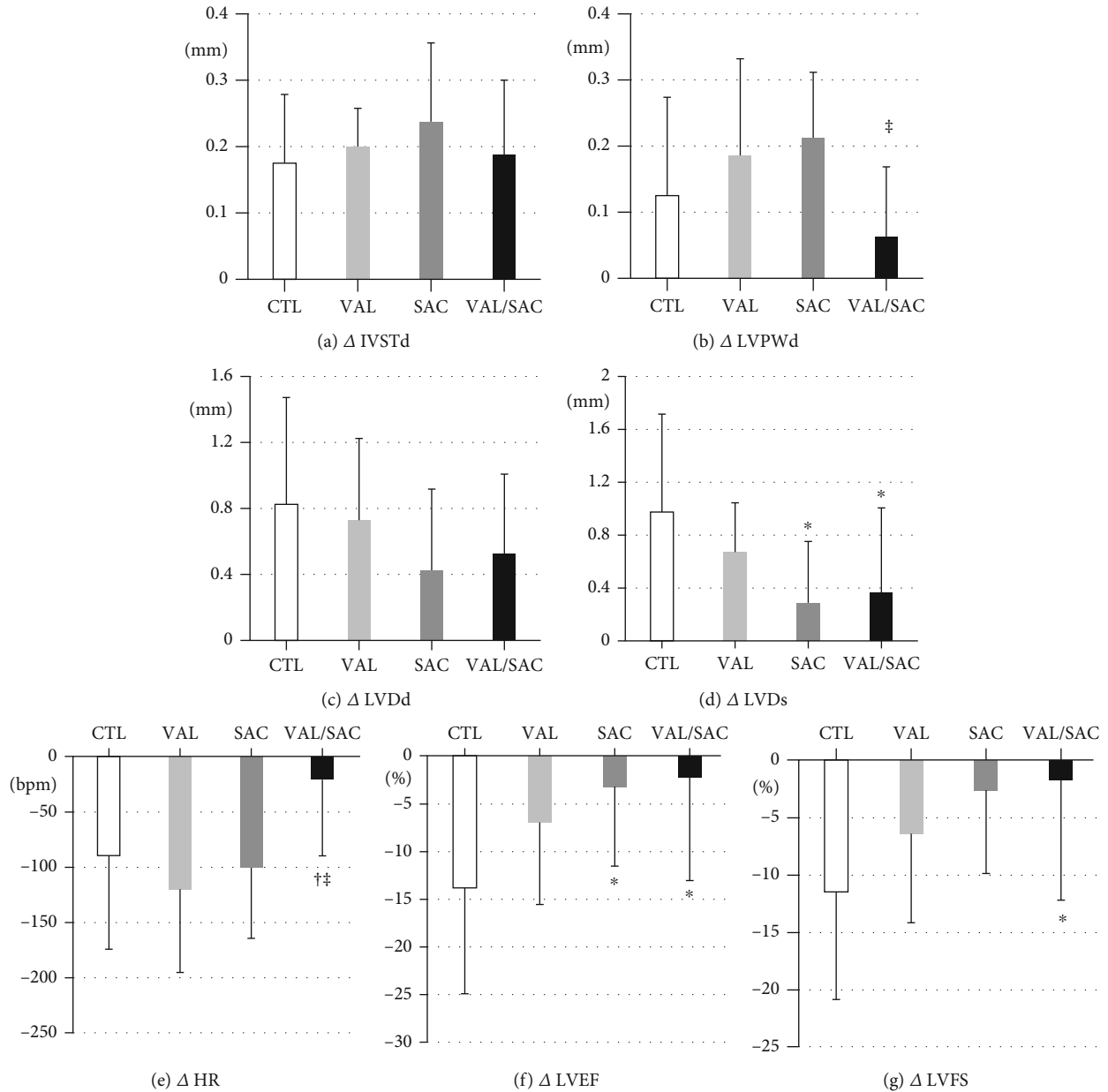


FIGURE 2: Changes in cardiac parameters via echocardiography after 12 weeks of treatment. Changes in (a) IVSTd, (b) LVPWd, (c) LVDDd, (d) LVDs, (e) HR, (f) LVEF, and (g) LVFS in each group. IVSTd: interventricular septum thickness diameter; LVPWd: left ventricular posterior wall thickness diameter; LVDDd: left ventricular internal dimension in diastole; LVDs: left ventricular internal dimension in systole; HR: heart rate; LVEF: left ventricular ejection fraction; LVFS: left ventricular fractional shortening; CTL: control group; VAL: valsartan group; SAC: sacubitril group; VAL/SAC: valsartan plus sacubitril group. CTL ($n=8$), VAL ($n=7$), SAC ($n=8$), and VAL/SAC ($n=8$) were investigated. *, †, and ‡ indicate significant differences compared with CTL, VAL, and SAC, respectively.

2.3. Quantitative Reverse Transcription-Polymerase Chain Reaction Analysis. mRNA expression levels were quantified using RT-PCR as previously described [18]. We extracted total ribonucleic acid from the apex of the left ventricle using a RiboPure RNA Purification Kit (Life Technologies, Carlsbad, CA, USA). We produced complementary deoxyribonucleic acid using a ReverTra Ace[®] qPCR RT Kit (TOYOBO, Japan). We performed quantitative RT-PCR on a 7500 Fast Real-Time PCR System (Applied Biosystems) using a THUNDERBIRD[®] SYBR[®] qPCR Mix (TOYOBO, Japan). We investigated natriuretic peptide type A (NPPA),

natriuretic peptide type B (NPPB), transforming growth factor- β (TGF- β), myosin heavy chain 7 (MyH7), CD34, vascular endothelial growth factor A (VEGFA), monocyte chemoattractant protein 1 (MCP1), gene of sarcoplasmic/endoplasmic reticulum calcium adenosine triphosphatase 2 (ATP2a2), vascular cell adhesion molecule-1 (VCAM-1), β catenin, vascular endothelial-cadherin (VE-cadherin), nuclear factor-kappa B (NF- κ B) inhibitor alpha (Nfkbia), inhibitor of NF- κ B kinase subunit beta (Ikkb), inhibitor of NF- κ B kinase regulatory subunit gamma (Ikkbg), lysosome-associated membrane glycoprotein 2 (Lamp2), phosphatase and tensin

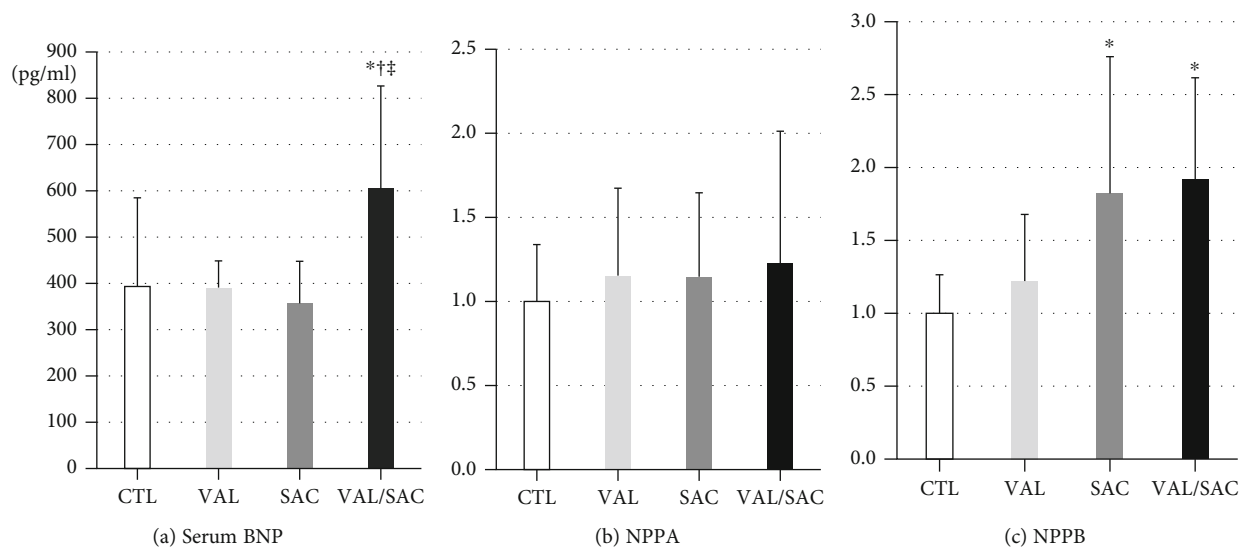


FIGURE 3: Serum BNP and mRNA expression levels of NPPA and NPPB in the LV. (a) Serum BNP levels and mRNA expression levels of (b) NPPA and (c) NPPB in each group. BNP: brain natriuretic peptide; NPPA: natriuretic peptide type A; NPPB: natriuretic peptide type B; CTL: control group; VAL: valsartan group; SAC: sacubitril group; VAL/SAC: valsartan plus sacubitril group. CTL ($n = 8$), VAL ($n = 7$), SAC ($n = 8$), and VAL/SAC ($n = 7$) were investigated. *, †, and ‡ indicate significant differences compared with CTL, VAL, and SAC, respectively.

homolog deleted on chromosome 10-induced kinase 1 (Pink1), and β actin in the left ventricle (LV). Table 1 lists the primers. Although we also investigated tumor necrosis factor α , interleukin-4, interleukin-6, interleukin-10, natriuretic peptide type C, plasminogen activator inhibitor 1, endothelial nitric oxide synthase, and endoplasmic reticulum oxidoreductin-1 in the LV, we could not analyze them due to low or undetectable expression. mRNA levels were expressed relative to mRNA levels of β actin, and the basal expression relative to that in the CTL group was considered to be 1.0.

2.4. Histological Analysis. We evaluated the quantity of myocardial fibrosis in Masson's trichrome-stained heart sections. Left ventricular tissues of the midlayer were fixed with 4% paraformaldehyde and stained with Masson's trichrome. The percentage of fibrotic area in the left ventricle was analyzed using the Image J software. To quantify myocardial angiogenesis, we stained fixed left ventricular tissues for immunohistochemical analysis of CD34. The percentage of CD34-positive cell area in the left ventricle was analyzed using the Image J software. Masson's trichrome staining and CD34 immunostaining were performed using Biopathology Institute Co. (Oita, Japan), and digital photographs were taken using a BZ-9000 series All-in-one Fluorescence Microscope (Keyence Japan, Osaka, Japan).

2.5. Statistical Analysis. All data analyses were performed using SAS (version 9.4, SAS Institute Inc., Cary, NC, USA) at Fukuoka University (Fukuoka, Japan), with a p value of <0.05 indicating statistical significance. Continuous variables were expressed as mean \pm standard deviation. Group differences were analyzed using a one-way analysis of variance.

3. Results

3.1. Changes in Body Weight and Blood Pressure. Figure 1 summarizes changes in body weight and blood pressure. Before prefeeding, the average baseline body weight and systolic blood pressure were 24.8 ± 1.6 g and 113.7 ± 12.2 mmHg, respectively. After 4 weeks of prefeeding, the average body weight and systolic blood pressure were 30.9 ± 1.9 g and 115.8 ± 14.6 mmHg, respectively. There were no significant differences between the groups. After 12 weeks of treatment, the average body weight and systolic blood pressure were 34.7 ± 4.3 g and 123.0 ± 18.3 mmHg, respectively. There were no significant differences between the treatment and CTL groups. None of the medications affected arterial blood pressure in the experimental animals.

3.2. Changes in Cardiac Functions. We investigated cardiac function using echocardiography at weeks 0 and 12 (Table 2). Figure 2 details the changes in cardiac parameters after 12 weeks of treatment. In the CTL group, LVDs increased by 0.98 ± 0.74 mm, whereas LVEF and LVFS decreased by $13.9\% \pm 11.1\%$ and $11.5\% \pm 9.4\%$, respectively, over 12 weeks. The VAL/SAC group showed a significantly smaller increase in LVDs (0.36 ± 0.64 mm; $p = 0.04$) and a significantly smaller decrease in LVEF ($2.25\% \pm 10.9\%$; $p = 0.03$) and LVFS ($1.8\% \pm 10.5\%$; $p = 0.04$) than the CTL group. The SAC group exhibited a significantly smaller increase in LVDs (0.29 ± 0.46 mm; $p = 0.03$) and a significantly smaller decrease in LVEF ($3.3\% \pm 8.3\%$; $p = 0.04$) than the CTL group.

3.3. Serum BNP and mRNA Expression Levels of NPPA and NPPB in the LV. Figure 3(a) presents serum BNP levels. After 12 weeks of treatment, the VAL/SAC group had significantly

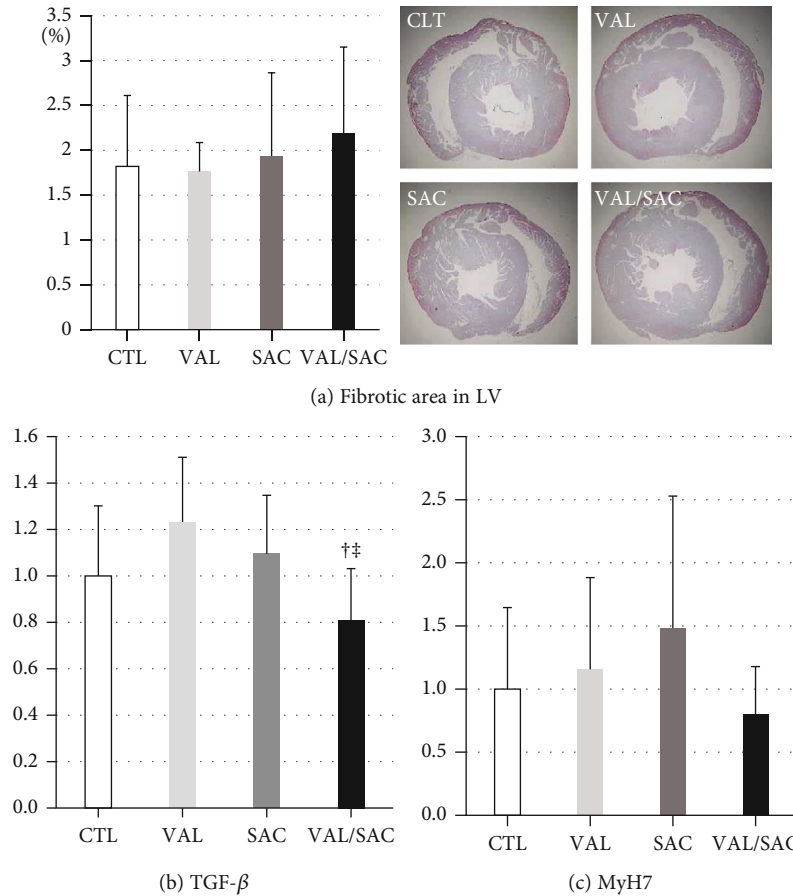


FIGURE 4: Cardiac fibrosis and hypertrophy in the LV. (a) Representative macrophotographs of the aorta with Masson's trichrome staining and quantification analysis for the percentage of fibrosis in each group. mRNA expression levels of (b) TGF- β and (c) MyH7 in each group are shown. TGF- β : transforming growth factor-beta; MyH7: myosin heavy chain 7; CTL: control group; VAL: valsartan group; SAC: sacubitril group; VAL/SAC: valsartan plus sacubitril group. CTL ($n = 8$), VAL ($n = 7$), SAC ($n = 8$), and VAL/SAC ($n = 7$) were investigated. \dagger and \ddagger indicate significant differences compared with VAL and SAC, respectively.

higher serum BNP levels than the CTL group (CTL: 393.2 ± 191.7 pg/mL and VAL/SAC: 605.2 ± 221.3 pg/mL, $p = 0.01$).

Figures 3(b) and 3(c) present detailed mRNA expression levels of NPPA and NPPB in the LV. The SAC and VAL/SAC groups had significantly higher expression levels of NPPB than the CTL group (SAC: 1.8 ± 0.9 times, $p = 0.02$ and VAL/SAC: 1.9 ± 0.7 times, $p = 0.01$) due to the effects of the neprilysin inhibitor. The neprilysin inhibitor did not increase NPPA expression in the LV since NPPA is mainly expressed in the atrium.

3.4. Cardiac Fibrosis and Hypertrophy in the LV. Considering our previous reports on the antifibrotic and hypertrophic effects of VAL/SAC [18, 19], we investigated cardiac fibrosis and hypertrophy in the LV. In this model, the CTL group showed only $1.8\% \pm 0.8\%$ fibrosis following histological analysis, with no significant differences between the groups (Figure 4(a)). After investigating mRNA expression levels of TGF- β (a marker of fibrosis) and MyH7 (a marker of hypertrophy) in the LV, the treatment groups did not show significantly better improvement than the CTL group (Figures 4(b) and 4(c)).

3.5. Regulation of NF- κ B and Lysosome Activity. We investigated the regulation of NF- κ B, mitochondrial activity in mitophagy, and lysosomal activity in autophagy (Figures 5(a)–5(e)). Accordingly, the VAL/SAC group had greater mRNA expression of Nfkbia, an NF- κ B inhibitor, than the CTL group (Figure 5(a)). Moreover, the VAL/SAC group showed greater expression of Lamp2, which plays a critical role in autophagosome maturation, than the CTL group (Figure 5(d)).

3.6. Angiogenic Effect. Figure 6(a) presents the results of histological analysis via CD34 immunostaining in the LV. Accordingly, there were no significant differences in the CD34-positive cell area in the LV between the groups. Figures 6(b)–6(h) show mRNA expression levels of markers of angiogenesis in the LV. The VAL/SAC group had significantly higher expression levels of CD34, VEGFA, MCP1, ATP2a2, and VCAM-1 but not β catenin or VE-cadherin (Figures 6(g) and 6(h)) than the CTL group (Figures 6(b)–6(f)).

4. Discussion

The present study showed that valsartan plus sacubitril increased myocardial angiogenic factors. The NF- κ B

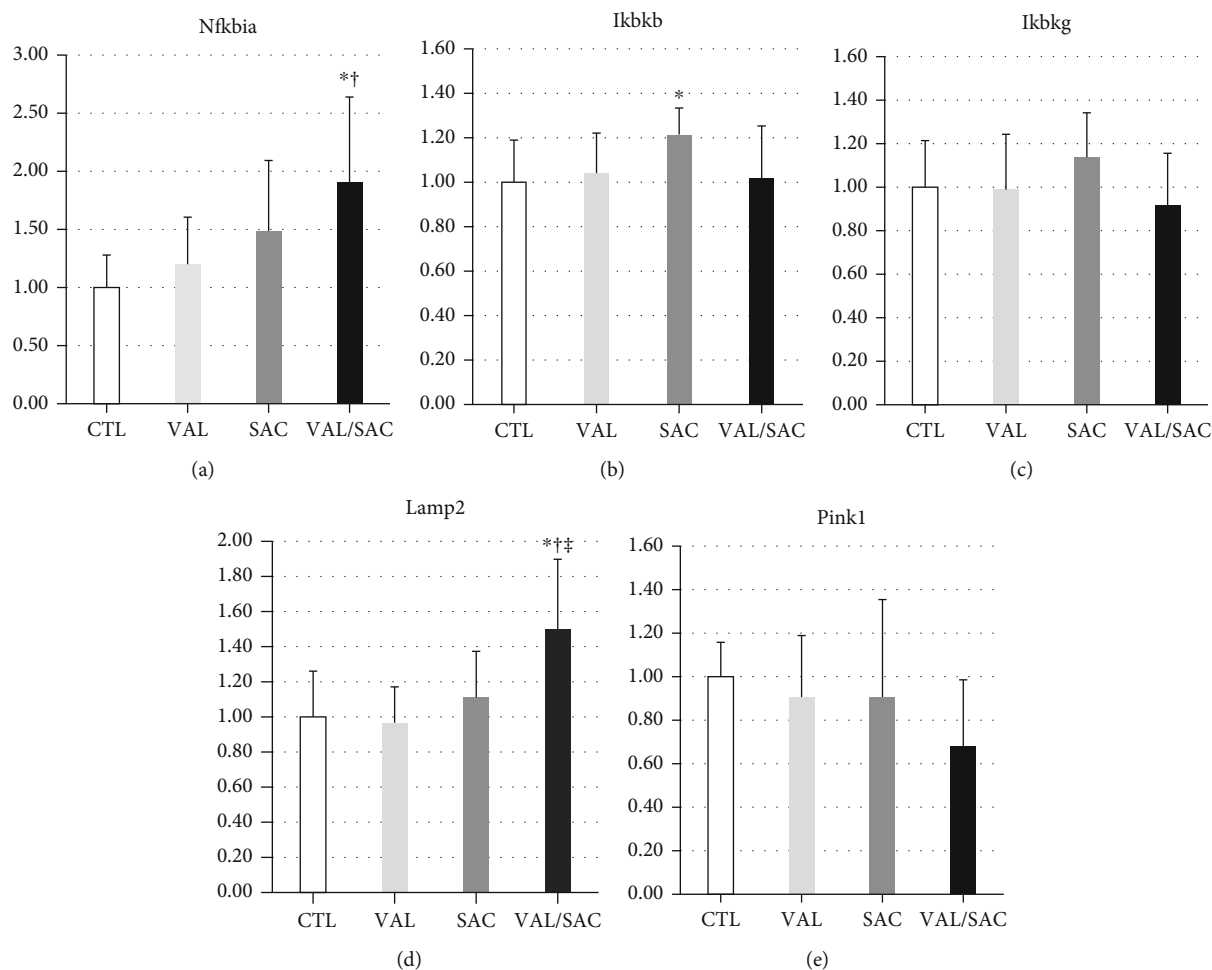


FIGURE 5: Regulation of NF- κ B and activity of mitochondria and lysosome. mRNA expression levels of (a) Nfkbia, (b) Ikbkb, (c) Ikbkg, (d) Lamp2, and (e) Pink1 in each group. NF- κ B: nuclear factor-kappa B; Nfkbia: NF- κ B inhibitor alpha; Ikbkb: an inhibitor of NF- κ B kinase subunit beta; Ikbkg: an inhibitor of NF- κ B kinase regulatory subunit gamma; Lamp2: lysosome-associated membrane glycoprotein 2; Pink1: phosphatase and tensin homolog deleted on chromosome 10-induced kinase 1; CTL: control group; VAL: valsartan group; SAC: sacubitril group; VAL/SAC: valsartan plus sacubitril group. CTL ($n=8$), VAL ($n=7$), SAC ($n=8$), and VAL/SAC ($n=7$) were investigated. *, †, and ‡ indicate significant differences compared with CTL, VAL, and SAC, respectively.

inhibitor preserved lysosomal activity and suppressed cardiac dysfunction in apolipoprotein E-knockout mice fed a high-fat diet independent of changes in cardiac fibrosis and hypertrophy in this model. Valsartan plus sacubitril demonstrated cardioprotective effects during early-stage cardiac dysfunction and ARNI might be useful for the primary prevention of heart failure via adaptation to the increase in oxygen demand.

Evidence showed that inhibition of the renin-angiotensin system promoted anti-inflammatory, antioxidant, and antifibrotic effects [29]. ARNI improved lymphatic system remodeling in a hypertrophic cardiomyopathy model [30] while decreasing oxidative stress and increasing adenosine triphosphate and Na⁺/K⁺-ATPase pump activity in ischemic reperfusion-induced arrhythmia [31]. However, no study has yet investigated the angiogenic effects of ARNI for adaptation to increased oxygen demand during cardiac hypertrophy.

Apolipoprotein E-knockout mice with or without a high-fat diet have been used to study atherosclerosis [32–36], plaque rupture [37], coronary artery disease [38], and cardiac

dysfunction [25–28]. Studies have shown that myocardial hypertrophy due to peripheral vascular resistance [25], hypertension and endothelial dysfunction [26], myocardial fibrosis [27], and reduced cardiac functional reserve cause cardiac dysfunction in apolipoprotein E-knockout mice [28]. Therefore, cardiac hypertrophy can be considered a cause of cardiac dysfunction in apolipoprotein E-knockout mice.

The myocardial angiogenic effects of ARNI occur in response to the increased oxygen demand under cardiac hypertrophy. Our model showed that blood pressure increased slightly, and that pathological proportion of fibrosis and mRNA expression of plasminogen activator inhibitor 1, a marker of fibrosis in the LV, remained low. The present study found that valsartan plus sacubitril did not exert any antihypertensive, antihypertrophic, or antifibrotic effects, probably due to the mild pathology in the animal model used herein. This finding may be attributable to the animals' young ages, short experimental periods, mild high-fat diet, or their interaction. Moreover, only slight changes in cardiac dysfunction parameters were observed in this model,

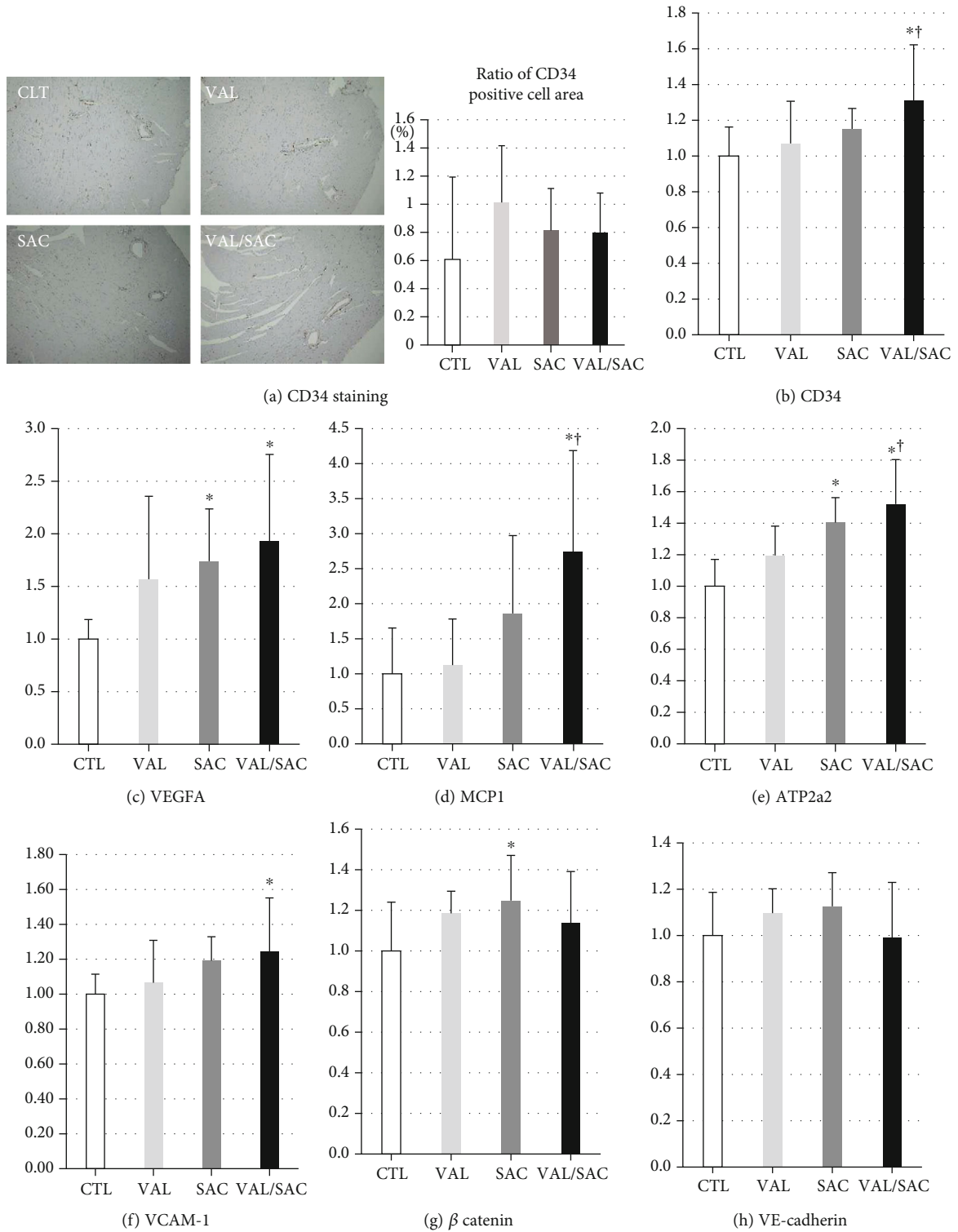


FIGURE 6: Myocardial angiogenesis. (a) Representative microphotographs of the left ventricle, with immunohistochemical staining for CD34, and a quantitative analysis for the percentage of the CD34-positive cell area in each group. mRNA expression levels of (b) CD34, (c) VEGFA, (d) MCP1, (e) ATP2a2, (f) VCAM-1, (g) β catenin, and (h) VE-cadherin in each group. CD34: clusters of differentiation 34; VEGFA: vascular endothelial growth factor A; MCP1: monocyte chemotactic protein 1; ATP2a2: gene name of sarcoplasmic/endoplasmic reticulum calcium adenosine triphosphatase 2; VCAM-1: vascular cell adhesion protein 1; VE-cadherin: vascular endothelial-cadherin; CTL: control group; VAL: valsartan group; SAC: sacubitril group; VAL/SAC: valsartan plus sacubitril group. CTL ($n = 8$), VAL ($n = 7$), SAC ($n = 8$), and VAL/SAC ($n = 7$) were investigated. *, †, and ‡ indicate significant differences compared with CTL, VAL, and SAC, respectively.

although valsartan plus sacubitril significantly suppressed the progression of cardiac dysfunction. The above results suggest that ARNI exerts cardioprotective effects in the early-stage of cardiac dysfunction, and that it can be useful for the primary prevention of heart failure onset during cardiac hypertrophy.

In this study, valsartan plus sacubitril increased serum BNP and mRNA expressions of NPPB in the LV, suppressed the dilation of LVDs, and preserved LVEF and LVFS. The PARADIGM-HF clinical trials showed that valsartan/sacubitril combination exerted cardioprotective effects against HFrEF [13]. Moreover, the US and European guidelines for HF management recommend valsartan/sacubitril combination as the first-line therapy for HFrEF [14, 15], with the present results being consistent with these recommendations. Our findings showed that one mechanism through which valsartan plus sacubitril exhibited cardioprotective effects was increased myocardial angiogenic factors. Based on our investigation, valsartan plus sacubitril increased mRNA expression levels of CD34, VEGFA, ATP2a2, and MCP1, all of which are myocardial angiogenic factors [39–42]. Autologous CD34-positive cell therapy for ischemic heart disease is associated with increased LVEF, exercise time, neovascularization, decreased angina, nitroglycerine use, heart failure, and mortality [43]. Meanwhile, ATP2a2 encodes sarcoplasmic/endoplasmic reticulum calcium adenosine triphosphatase 2 (SERCA2a). Cardiac SERCA2a has been associated with myocardial angiogenesis [40] and calcium recycling of the cardiac muscle [44], which is another therapeutic target for heart failure [45]. Increasing mRNA expression of ATP2a2 through valsartan plus sacubitril treatment might improve cardiac dysfunction through calcium recycling independent of myocardial angiogenesis. However, the present study did not investigate the detailed pathway of calcium recycling. Moreover, our findings showed that the valsartan plus sacubitril group had low mRNA expression levels of inflammatory markers, including tumor necrosis factor α and interleukin-6, but high mRNA expression levels of MCP1. After investigating anti-inflammatory markers, including interleukin-4 and interleukin-10, our findings showed that both had low mRNA expression levels. Our model showed that valsartan plus sacubitril did not have anti-inflammatory or inflammatory effects in the LV.

In the chronic phase, prolonged activation of NF- κ B is cytotoxic and promotes heart failure by triggering an inflammatory response [46]. NF- κ B is also a good regulator of cardiac hypertrophy [47]. Our findings showed that valsartan plus sacubitril increased the mRNA expression of Nfkbia, one of the main inhibitors of NF- κ B, suggesting that ARNI can regulate NF- κ B during early-stage cardiac dysfunction. Optimal autophagic activity is critical in the maintenance of cardiovascular homeostasis and function [48]. Autophagic or mitophagic flux in the cardiovascular system has been associated with the spontaneous development of cardiovascular disorders [49]. Lamp2 is a critical protein for autophagic flux. Danon disease, which occurs due to loss of function mutations in the Lamp2 gene, causes impaired mitophagy, facilitating mitochondrial damage [50]. The valsartan plus

sacubitril group included herein showed high mRNA expression of Lamp2, which might be one of the effects of valsartan and sacubitril for early-stage cardiac dysfunction.

The present study has several limitations worth noting. First, older apolipoprotein E-knockout mice, a longer experimental period, and a higher-fat diet should have been used to investigate hypertension and cardiac fibrosis during cardiac hypertrophy. However, given the fact that our focus was on the angiogenic effects of valsartan plus sacubitril for early-stage cardiac dysfunction, our model can be deemed appropriate for this study. Second, our CD34 immunostaining analysis showed no valsartan plus sacubitril-induced enhancement of myocardial angiogenesis. Although ARNI in another animal model [51] and natriuretic peptide [52–54] reportedly exhibited angiogenic effects, some studies show that natriuretic peptide suppresses angiogenesis [55, 56]. However, the present study found considerably low mRNA levels of endothelial markers in the LV, including endothelial nitric oxide synthase, endoplasmic reticulum oxidoreductin-1, and NPPC. Such discrepant outcomes need to be carefully considered in future studies, together with the use of other animal models in the investigation of myocardial angiogenesis and endothelial markers in the heart.

5. Conclusions

The present study showed that valsartan plus sacubitril preserved left ventricular systolic function in apolipoprotein E-knockout mice fed a high-fat diet. The ARNI-induced myocardial angiogenic factors possibly explain its cardioprotective effects.

Data Availability

No data were used to support this study.

Disclosure

This research was presented at the Joint Meeting ESH-ISH 2021 and published the abstract in the Journal of Hypertension (doi:10.1097/01.hjh.0000746572.65667.fd).

Conflicts of Interest

The authors declare that they have no conflicts of interest.

Acknowledgments

This work was supported in part by funds (No. 187203) from the Central Research Institute of Fukuoka University, a grant from The Clinical Research Promotion Foundation (2018), and JSPS KAKENHI Grant Number JP19K17618. We thank Kanji Nakai, Sayo Tomita, and Satomi Abe for their excellent technical assistance.

References

- [1] R. S. Vasan, “Cardiac function and obesity,” *Heart*, vol. 89, no. 10, pp. 1127–1129, 2003.

- [2] M. Iemitsu, T. Miyauchi, S. Maeda et al., "Physiological and pathological cardiac hypertrophy induce different molecular phenotypes in the rat," *American Journal of Physiology. Regulatory, Integrative and Comparative Physiology*, vol. 281, no. 6, pp. R2029–R2036, 2001.
- [3] U. Varma, P. Koutsifeli, V. L. Benson, K. M. Mellor, and L. M. D. Delbridge, "Molecular mechanisms of cardiac pathology in diabetes - experimental insights," *Biochimica et Biophysica Acta - Molecular Basis of Disease*, vol. 1864, no. 5, pp. 1949–1959, 2018.
- [4] A. A. Gibb and B. G. Hill, "Metabolic coordination of physiological and pathological cardiac remodeling," *Circulation Research*, vol. 123, no. 1, pp. 107–128, 2018.
- [5] S. Isoyama, N. Ito, M. Komatsu et al., "Responses to hemodynamic stress in the aged heart," *Japanese Heart Journal*, vol. 35, no. 4, pp. 403–418, 1994.
- [6] A. Marino, Y. Zhang, L. Rubinelli, M. A. Riemma, J. E. Ip, and A. di Lorenzo, "Pressure overload leads to coronary plaque formation, progression, and myocardial events in ApoE^{-/-} mice," *JCI Insight*, vol. 4, no. 9, 2019.
- [7] T. Oka, H. Akazawa, A. T. Naito, and I. Komuro, "Angiogenesis and cardiac hypertrophy: maintenance of cardiac function and causative roles in heart failure," *Circulation Research*, vol. 114, no. 3, pp. 565–571, 2014.
- [8] B. Ferraro, G. Leoni, R. Hinkel et al., "Pro-angiogenic macrophage phenotype to promote myocardial repair," *Journal of the American College of Cardiology*, vol. 73, no. 23, pp. 2990–3002, 2019.
- [9] M. Kumagai, K. Minakata, H. Masumoto et al., "A therapeutic angiogenesis of sustained release of basic fibroblast growth factor using biodegradable gelatin hydrogel sheets in a canine chronic myocardial infarction model," *Heart and Vessels*, vol. 33, no. 10, pp. 1251–1257, 2018.
- [10] T. Matsumoto, S. Yamashita, S. Yoshino et al., "Therapeutic arteriogenesis/angiogenesis for peripheral arterial disease by nanoparticle-mediated delivery of pitavastatin into vascular endothelial cells," *Annals of Vascular Diseases*, vol. 13, no. 1, pp. 4–12, 2020.
- [11] A. Bayes-Genis, J. Barallat, and A. M. Richards, "A test in context: neprilysin: function, inhibition, and biomarker," *Journal of the American College of Cardiology*, vol. 68, no. 6, pp. 639–653, 2016.
- [12] M. Volpe, S. Rubattu, and A. Battistoni, "ARNi: a novel approach to counteract cardiovascular diseases," *International Journal of Molecular Sciences*, vol. 20, no. 9, p. 2092, 2019.
- [13] J. J. McMurray, M. Packer, A. S. Desai et al., "Angiotensin-neprilysin inhibition versus enalapril in heart failure," *The New England Journal of Medicine*, vol. 371, no. 11, pp. 993–1004, 2014.
- [14] P. Ponikowski, A. A. Voors, S. D. Anker et al., "2016 ESC Guidelines for the diagnosis and treatment of acute and chronic heart failure: the Task Force for the diagnosis and treatment of acute and chronic heart failure of the European Society of Cardiology (ESC). Developed with the special contribution of the Heart Failure Association (HFA) of the ESC," *European Journal of Heart Failure*, vol. 18, no. 8, pp. 891–975, 2016.
- [15] C. W. Yancy, M. Jessup, B. Bozkurt et al., "2017 ACC/AHA/HFSA focused update of the 2013 ACCF/AHA guideline for the management of heart failure: a report of the American College of Cardiology/American Heart Association Task Force on Clinical Practice Guidelines and the Heart Failure Society of America," *Circulation*, vol. 136, no. 6, pp. e137–e161, 2017.
- [16] D. H. Kang, S. J. Park, S. H. Shin et al., "Angiotensin receptor neprilysin inhibitor for functional mitral regurgitation," *Circulation*, vol. 139, no. 11, pp. 1354–1365, 2019.
- [17] J. L. Januzzi, J. Butler, E. Fombu et al., "Rationale and methods of the Prospective Study of Biomarkers, Symptom Improvement, and Ventricular Remodeling During Sacubitril/Valsartan Therapy for Heart Failure (PROVE-HF)," *American Heart Journal*, vol. 199, pp. 130–136, 2018.
- [18] Y. Suematsu, S. Miura, M. Goto et al., "LCZ696, an angiotensin receptor-neprilysin inhibitor, improves cardiac function with the attenuation of fibrosis in heart failure with reduced ejection fraction in streptozotocin-induced diabetic mice," *European Journal of Heart Failure*, vol. 18, no. 4, pp. 386–393, 2016.
- [19] Y. Suematsu, W. Jing, A. Nunes et al., "LCZ696 (sacubitril/valsartan), an angiotensin-receptor neprilysin inhibitor, attenuates cardiac hypertrophy, fibrosis, and vasculopathy in a rat model of chronic kidney disease," *Journal of Cardiac Failure*, vol. 24, no. 4, pp. 266–275, 2018.
- [20] W. Jing, N. D. Vaziri, A. Nunes et al., "LCZ696 (sacubitril/valsartan) ameliorates oxidative stress, inflammation, fibrosis and improves renal function beyond angiotensin receptor blockade in CKD," *American Journal of Translational Research*, vol. 9, no. 12, pp. 5473–5484, 2017.
- [21] S. I. Miura, Y. Suematsu, Y. Matsuo et al., "The angiotensin II type 1 receptor-neprilysin inhibitor LCZ696 blocked aldosterone synthesis in a human adrenocortical cell line," *Hypertension Research*, vol. 39, no. 11, pp. 758–763, 2016.
- [22] S. Andersen, J. B. Axelsen, S. Ringgaard et al., "Effects of combined angiotensin II receptor antagonism and neprilysin inhibition in experimental pulmonary hypertension and right ventricular failure," *International Journal of Cardiology*, vol. 293, pp. 203–210, 2019.
- [23] T. Seki, K. Goto, Y. Kansui, T. Ohtsubo, K. Matsumura, and T. Kitazono, "Angiotensin II receptor-neprilysin inhibitor sacubitril/valsartan improves endothelial dysfunction in spontaneously hypertensive rats," *Journal of the American Heart Association*, vol. 6, no. 10, 2017.
- [24] H. Zhang, G. Liu, W. Zhou, W. Zhang, K. Wang, and J. Zhang, "Neprilysin inhibitor-angiotensin II receptor blocker combination therapy (sacubitril/valsartan) suppresses atherosclerotic plaque formation and inhibits inflammation in apolipoprotein E-deficient mice," *Scientific Reports*, vol. 9, no. 1, p. 6509, 2019.
- [25] C. J. Hartley, A. K. Reddy, S. Madala et al., "Hemodynamic changes in apolipoprotein E-knockout mice," *American Journal of Physiology. Heart and Circulatory Physiology*, vol. 279, no. 5, pp. H2326–H2334, 2000.
- [26] R. Yang, L. Powell-Braxton, A. K. Ogaoawara et al., "Hypertension and endothelial dysfunction in apolipoprotein E knockout mice," *Arteriosclerosis, Thrombosis, and Vascular Biology*, vol. 19, no. 11, pp. 2762–2768, 1999.
- [27] K. L. Ma, J. Liu, J. Ni et al., "Inflammatory stress exacerbates the progression of cardiac fibrosis in high-fat-fed apolipoprotein E knockout mice via endothelial-mesenchymal transition," *International Journal of Medical Sciences*, vol. 10, no. 4, pp. 420–426, 2013.
- [28] J. Vincelette, B. Martin-McNulty, R. Vergona, M. E. Sullivan, and Y. X. Wang, "Reduced cardiac functional reserve in apolipoprotein E knockout mice," *Translational Research*, vol. 148, no. 1, pp. 30–36, 2006.

- [29] E. Ahmadian, P. S. Pennefather, A. Eftekhari, et al. R. Heidari, and M. A. Eghbal, "Role of renin-angiotensin system in liver diseases: an outline on the potential therapeutic points of intervention," *Expert Review of Gastroenterology & Hepatology*, vol. 10, no. 11, pp. 1279–1288, 2016.
- [30] Q. Ge, L. Zhao, C. Liu et al., "LCZ696, an angiotensin receptor-nephrilysin inhibitor, improves cardiac hypertrophy and fibrosis and cardiac lymphatic remodeling in transverse aortic constriction model mice," *BioMed Research International*, vol. 2020, Article ID 7256862, 10 pages, 2020.
- [31] T. M. Abdulsalam, A. H. Hasanin, R. H. Mohamed, and A. el Sayed Badawy, "Angiotensin receptor-nephrilysin inhibitor (thiorphan/irbesartan) decreased ischemia-reperfusion induced ventricular arrhythmias in rat; in vivo study," *European Journal of Pharmacology*, vol. 882, p. 173295, 2020.
- [32] S. H. Zhang, R. L. Reddick, J. A. Piedrahita, and N. Maeda, "Spontaneous hypercholesterolemia and arterial lesions in mice lacking apolipoprotein E," *Science*, vol. 258, no. 5081, pp. 468–471, 1992.
- [33] S. Ding, J. Jiang, P. Yu, G. Zhang, G. Zhang, and X. Liu, "Green tea polyphenol treatment attenuates atherosclerosis in high-fat diet-fed apolipoprotein E-knockout mice via alleviating dyslipidemia and up-regulating autophagy," *PLoS One*, vol. 12, no. 8, article e0181666, 2017.
- [34] Y. K. Chan, M. S. Brar, P. V. Kirjavainen et al., "High fat diet induced atherosclerosis is accompanied with low colonic bacterial diversity and altered abundances that correlates with plaque size, plasma A-FABP and cholesterol: a pilot study of high fat diet and its intervention with *Lactobacillus rhamnosus* GG (LGG) or telmisartan in ApoE(-/-) mice," *BMC Microbiology*, vol. 16, no. 1, p. 264, 2016.
- [35] L. Xiao, L. Liu, X. Guo et al., "Quercetin attenuates high fat diet-induced atherosclerosis in apolipoprotein E knockout mice: a critical role of NADPH oxidase," *Food and Chemical Toxicology*, vol. 105, pp. 22–33, 2017.
- [36] A. Stachowicz, A. Wiśniewska, K. Kuś et al., "The influence of trehalose on atherosclerosis and hepatic steatosis in apolipoprotein E knockout mice," *International Journal of Molecular Sciences*, vol. 20, no. 7, p. 1552, 2019.
- [37] A. R. Bond and C. L. Jackson, "The fat-fed apolipoprotein E knockout mouse brachiocephalic artery in the study of atherosclerotic plaque rupture," *Journal of Biomedicine & Biotechnology*, vol. 2011, Article ID 379069, 10 pages, 2011.
- [38] T. Yamashita, S. Kawashima, M. Ozaki et al., "In vivo angiographic detection of vascular lesions in apolipoprotein E-knockout mice using a synchrotron radiation microangiography system," *Circulation Journal*, vol. 66, no. 11, pp. 1057–1059, 2002.
- [39] J. Fan, H. Li, X. Nie et al., "MiR-665 aggravates heart failure via suppressing CD34-mediated coronary microvessel angiogenesis," *Aging (Albany NY)*, vol. 10, no. 9, pp. 2459–2479, 2018.
- [40] J. P. Laakkonen, J. Lähteenvuuo, S. Jauhiainen, T. Heikura, and S. Ylä-Herttua, "Beyond endothelial cells: vascular endothelial growth factors in heart, vascular anomalies and placenta," *Vascular Pharmacology*, vol. 112, pp. 91–101, 2019.
- [41] Y. Mei, M. D. Thompson, Y. Shiraishi, R. A. Cohen, and X. Tong, "Sarcoplasmic/endoplasmic reticulum Ca^{2+} ATPase C674 promotes ischemia- and hypoxia-induced angiogenesis via coordinated endothelial cell and macrophage function," *Journal of Molecular and Cellular Cardiology*, vol. 76, pp. 275–282, 2014.
- [42] H. Morimoto and M. Takahashi, "Role of monocyte chemoattractant protein-1 in myocardial infarction," *International Journal of Biomedical Sciences*, vol. 3, pp. 159–167, 2007.
- [43] W. K. Sietsema, A. Kawamoto, H. Takagi, and D. W. Losordo, "Autologous CD34+ cell therapy for ischemic tissue repair," *Circulation Journal*, vol. 83, no. 7, pp. 1422–1430, 2019.
- [44] M. A. Shareef, L. A. Anwer, and C. Poizat, "Cardiac SERCA2A/B: therapeutic targets for heart failure," *European Journal of Pharmacology*, vol. 724, pp. 1–8, 2014.
- [45] L. Lipskaia, E. R. Chemaly, L. Hadri, A. M. Lompre, and R. J. Hajjar, "Sarcoplasmic reticulum Ca^{2+} ATPase as a therapeutic target for heart failure," *Expert Opinion on Biological Therapy*, vol. 10, no. 1, pp. 29–41, 2010.
- [46] J. W. Gordon, J. A. Shaw, and L. A. Kirshenbaum, "Multiple facets of NF- κ B in the Heart," *Circulation Research*, vol. 108, no. 9, pp. 1122–1132, 2011.
- [47] A. Fiordelisi, G. Iaccarino, C. Morisco, E. Coscioni, and D. Sorriento, "NF κ B is a key player in the crosstalk between inflammation and cardiovascular diseases," *International Journal of Molecular Sciences*, vol. 20, no. 7, p. 1599, 2019.
- [48] S. Lavandro, M. Chiong, B. A. Rothermel, and J. A. Hill, "Autophagy in cardiovascular biology," *The Journal of Clinical Investigation*, vol. 125, no. 1, pp. 55–64, 2015.
- [49] J. M. Bravo-San Pedro, G. Kroemer, and L. Galluzzi, "Autophagy and mitophagy in cardiovascular disease," *Circulation Research*, vol. 120, no. 11, pp. 1812–1824, 2017.
- [50] S. I. Hashem, A. N. Murphy, A. S. Divakaruni et al., "Impaired mitophagy facilitates mitochondrial damage in Danon disease," *Journal of Molecular and Cellular Cardiology*, vol. 108, pp. 86–94, 2017.
- [51] D. Pfau, S. L. Thorn, J. Zhang et al., "Angiotensin receptor neprilysin inhibitor attenuates myocardial remodeling and improves infarct perfusion in experimental heart failure," *Scientific Reports*, vol. 9, no. 1, article 5791, 2019.
- [52] H. Chen, Y. C. Levine, D. E. Golan, T. Michel, and A. J. Lin, "Atrial Natriuretic Peptide-initiated cGMP Pathways Regulate Vasodilator-stimulated Phosphoprotein Phosphorylation and Angiogenesis in Vascular Endothelium," *The Journal of Biological Chemistry*, vol. 283, no. 7, pp. 4439–4447, 2008.
- [53] M. Kuhn, K. Völker, K. Schwarz et al., "The natriuretic peptide/guanylyl cyclase—a system functions as a stress-responsive regulator of angiogenesis in mice," *The Journal of Clinical Investigation*, vol. 119, no. 7, pp. 2019–2030, 2009.
- [54] K. J. Bubb, A. A. Aubdool, A. J. Moyes et al., "Endothelial C-type natriuretic peptide is a critical regulator of angiogenesis and vascular remodeling," *Circulation*, vol. 139, no. 13, pp. 1612–1628, 2019.
- [55] A. Pedram, M. Razandi, and E. R. Levin, "Natriuretic peptides suppress vascular endothelial cell growth factor signaling to angiogenesis," *Endocrinology*, vol. 142, no. 4, pp. 1578–1586, 2001.
- [56] N. Lara-Castillo, S. Zandi, S. Nakao et al., "Atrial natriuretic peptide reduces vascular leakage and choroidal neovascularization," *The American Journal of Pathology*, vol. 175, no. 6, pp. 2343–2350, 2009.